RESEARCH ARTICLE | FEBRUARY 16 2024

Thermal diffusivity modeling for aluminum AA6060 plates during friction stir welding

M. Serier; Raad Jamal Jassim; Raheem Al-Sabur ✉; A. N. Siddiquee

AIP Conf. Proc. 3051, 070004 (2024)
https://doi.org/10.1063/5.0191742

Thermal Diffusivity Modeling for Aluminum AA6060 Plates During Friction Stir Welding

M. Serier[1, a)], Raad Jamal Jassim[2, b)], Raheem Al-Sabur[2,c)] and A. N. Siddiquee[3, d)]

[1]*Mechanical Engineering Department, University of Ain Temouchent, Ain Temouchent 46000, Algeria*
[2]*Mechanical Engineering Department, University of Basrah, Basrah 61001, Iraq*
[3]*Mechanical Engineering Department, Jamia Millia Islamia, New Delhi110025, India*

[a)] mohamed.serier@univ-temouchent.edu.dz
[b)] raad.jassim@uobasrah.edu.iq
[c)] Corresponding author: raheem.musawel@uobasrah.edu.iq
[d)] arshadnsiddiqui@gmail.com

Abstract. In the last three decades, a significant turning point occurred in the history of welding technology through friction stir welding (FSW) technology. As a solid-state welding, FSW successfully welded similar metals and extended them to include welding of dissimilar materials, composites, and polymers. Heat diffusivity affects the weld heat generated and, thus, the heat-affected zone's nature and the weld joint's efficiency. In this article, the thermal diffusivity of AA6060-T5 aluminum alloy welded was modelled by FSW, and experimental results verified the results. The study proved that thermal diffusivity is an essential factor in the performance of this type of alloy during FSW. The weld zone's thermal conductivity and density decrease slightly with increasing temperature. Furthermore, to obtain a good weld joint, the thermal diffusivity must be reduced, which is done by keeping the melting temperature of the metal in the HAZ zone. Furthermore, The temperature of the A 6060-T5 aluminum just below the FSW tool shoulder can approach its melting temperature when a forging force of 5 KN is applied.

Keywords. FSW, thermal diffusivity, friction stir welding, aluminum.

INTRODUCTION

Friction stir welding (FSW) is one of the most researched processes since it was invented nearly three decades ago[1]. This intensive research led to significant improvements in the process capabilities and developments of its new variant, which rapidly enhanced its adoption by the industry due to a steady increase in its applications. The process was initially invented for aerospace applications, but it evolved as a versatile process and is no longer confined to the aerospace industry. The expansion of its application to various sectors and a significant rise in the FSW tool and tooling manufacturing (such as vibration-assisted tools)[2]. Furthermore, among prominent FSW variants, friction stir processing (FSP) has evolved as generic processing technology, and friction stir spot welding (FSSW) competes strongly with resistance spot welding due to low energy consumption, classifying it among the important sustainable manufacturing routes [3]. FSW's success was not limited to competing with fusion welding but extended to effectively joining dissimilar metals and composite materials. Also, attempts to weld polymeric materials such as polyvinyl chloride (PVC), nylon-6 (PA 6), and HDPE also gave promising results [4]. Apart from parametric investigations, several strategies have also produced interesting results in FSW, including under different cooling media, additive manufacturing and in-situ alloying. The cons-intensive FSW setup also led to cost-effective retrofitting and portable FSW system development [5, 6]. There are extensive studies on finding the optimum parameters of the FSW for different materials and tool designs[7] or studying specific conditions such as FSW underwater[8]. Apart from cost-intensive setup, tool design and developments, preparations of welding ready plate and high tool/work setup time are other major limitations of the FSW. The modelling and simulations effectively

3rd International Conference on Engineering and Science
AIP Conf. Proc. 3051, 070004-1–070004-9; https://doi.org/10.1063/5.0191742
Published by AIP Publishing. 978-0-7354-4808-7/$30.00

reduce the time and cost of the FSW welds. This necessitated modelling, and several works on thermal, heat input, residual stress, flow and force modelling have been reported. The rate at which a body with an irregular temperature approaches its equilibrium state is known as thermal diffusivity. The thermal diffusivity, which is calculated as the ratio of thermal conductivity to specific heat capacity and density at constant pressure[9]. Thermal diffusivity is a crucial factor in welding processes, especially in FSW, but work on this important aspect is reported less.

The effect of thermal diffusivity has been experimentally investigated in some previous studies. B. Kulkarni et al. indicated that understanding the relationship between thermal diffusivity and plastic deformation is crucial for optimizing the processing parameters and achieving the desired properties in materials with low thermal diffusivity, which limits plastic deformation for metals like copper in FSW [10]. W. J. Choi et al. [11].suggested increasing the rotational speed to avoid the low rates of plastic deformation in the FSW, but this leads to a weak weld joint and increases the possibility of corrosion later [11]. Zhang et al. [12] completed comprehensive FSW experimental studies about the relationship between the friction coefficient and the process parameters. They found that local temperatures significantly influence the resulting friction coefficients. Jae-Ha Kim et al.[13] compared the effect of several FSW passes on the thermal diffusivity variation for the Ag-CNT/Cu and CNT/Cu composites and pure copper. They indicated that the thermal diffusivity of the CNT/Cu and Cu was lower than the Ag-CNT/Cu as composite, whereas it was increased at 100°C up to 118 mm2/s using two passes of FSW. Igor Zybin et al. [14] established that thermal diffusivity plays a crucial role in the successful FSW process of AA 5056. Their research further sheds light on the impact of root side thermal boundary conditions on welding process variables and the resulting properties of FSW joints. A K Singh et al. [15] conducted an experimental study to investigate the influence of thermal diffusivity on stir zone formation during the friction stir welding (FSW) of AA6061-T6 and magnesium AZ31 alloy. They employed a laser flash method to compare the thermal diffusivity of five joint sets within a specified temperature range. Their findings revealed that the resulting thermal diffusivity varies with changes in shoulder diameters. Bhardwaj Kulkarni et al. [16] investigated the impact of the backing plate on the corrosion rates of FSW joints. They examined the thermal diffusivity of AA6061 backing plates by employing the exfoliation corrosion test to assess the corrosion resistance of the welds. Their findings suggested that controlling corrosion rates is possible by using specific values for welding parameters.

The thermal diffusivity of the backing plate during the joining of AA6056 sheets by FSW was studied by Upadhyay et al. [17], and produced interesting results showed that the thermal conductivity has a significant effect on the formation of the nugget zone, which is related to achieve peak temperature during the FSW.

The effect of thermal diffusivity was numerically investigated using the FSW process modelling. Researchers were still working on modelling the FSW process three decades ago. Frigaard et al. [18] were among the first to model this process, as they considered that it consists of four periods: heating, pseudo-steady state, transient heating, and the post-steady state periods. In the fourth period, the heat reaction from the end plate surface leads to an additional heat buildup around the tool shoulder and influences the heat-affected zone (HAZ).

With advances in computers and the availability of commercial software, the finite difference method (FDM) and finite element method (FEM) have been used instead of analytical approaches for FSW modelling. Song and Kovacevic [19] also used Rosenthal's analytical method and FDM for FSW heat source modelling but neglected the generated heat of the plastic deformation between the workpiece and the tool pin. José Cintra Filho et al. [20] used FDM to develop equations for thermo-mechanical modelling and describe the behaviour of experimentally measured temperatures of AA2024-T3 aluminum alloy during the FSW process. Buffa et al. [21] used the DEFORM-3D software based on an implicit Lagrangian approach to predict the strain rate and material flow and study the temperature profile during the FSW process. The investigations reported on the thermal diffusivity were focused primarily on the material being welded and consolidated under the FSW tool.

The purpose of this maiden research is to model the variation of the heat diffusion generated between the tool and aluminum alloy plates as a function of welding time, as well as the rate of change of thermal diffusivity within the material being consolidated into a joint and its constituent factors simultaneously with the movement of the tool along the welding joint.

METHODOLOGY

Mathematical Modeling Analysis

An accurate understanding of the flux capacity absorbed by welded sheets is necessary to solve the thermal problem during FSW. Heat input during the FSW process is sourced from the friction between the pin and shoulder surfaces of the FSW tool and the work material being joined (as shown in Fig. 1). The FSW tool provides three interfaces: two for (a) shoulder and (b) bottom surface of the pin, and the third (c) for a threaded cylindrical lateral profile of the pin. The interfaces are required for effective plastic deformation of the material, sufficient material flow, and generating the required heat for welding.

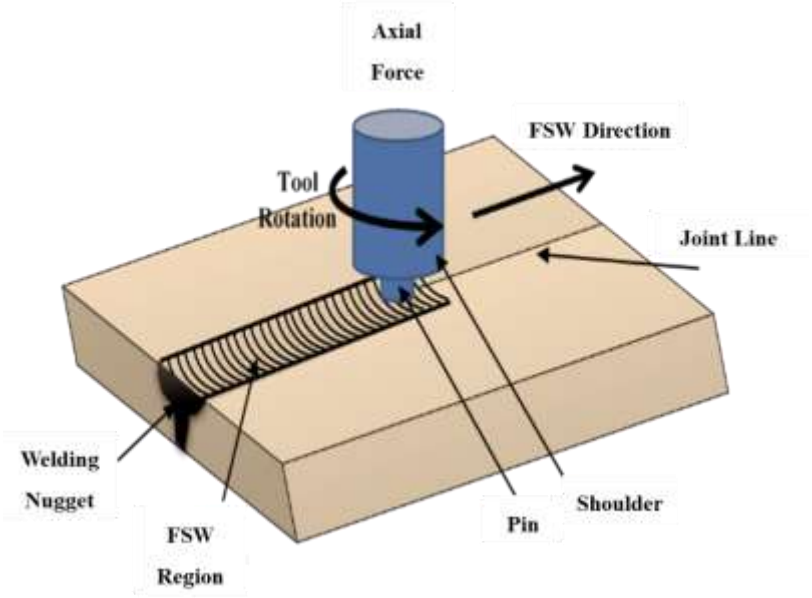

FIGURE 1. FSW Process Schematic

Thermal modelling is often based on the welding heat sources in FSW, which is essential for better understanding the material flow. All thermal, analytical, or numerical modelling in FSW depends on the thermal conductivity equation, considering the appropriate boundary conditions[19].

The present thermal model using 3D heat transfer computations utilized several simplifying assumptions, such as the majority assuming the pin shape is cylindrical and the problem is considered quasi-stationary of the conduction/convection type of movable coordinate system (o, x, y, z) [22]. In addition, the maximum temperature is always less than the melting point Tf, and the losses from the material's surfaces are through natural convection. Furthermore, the heat generated by the FSW tool's plastic deformation is assumed to be negligible compared to the heat generated by friction and plastic deformation of the workpiece materials.

With the above assumptions and the moving coordinate system, the heat transfer equation during welding can be written as follows [19]:

$$\left(\frac{\partial \rho cT}{\partial t}\right) = \frac{\partial}{\partial x}\left(k_x \frac{\partial T}{\partial x}\right) + \frac{\partial}{\partial y}\left(k_y \frac{\partial T}{\partial y}\right) + \frac{\partial}{\partial z}\left(k_z \frac{\partial T}{\partial z}\right) + S + \omega_v \frac{\partial (\rho cT)}{\partial x} \quad (1)$$

The temperature (T) in friction stir welding (FSW) is influenced by heating capacity (c), density (ρ), and heat conductivities (kx, ky, kz) along respective axes, as well as the volumetric source (S) and welding speed. Although the volumetric source is negligible compared to the main heat source resulting from friction, the conduction and convection coefficients on various surfaces still play a crucial role in determining the thermal history of the workpiece during FSW.

Heat Source Model

The heat input during welding is delivered from the pin/workpiece interface and the shoulder/workpiece interface. The heat generated at the pin/workpiece interface comprises three parts[23], as shown in Fig. 2:

1. The heat generated by the material's shearing (i.e., plastic deformation).
2. The heat is generated by friction on the pin lateral profile.
3. The heat is generated by friction on the pin bottom face.

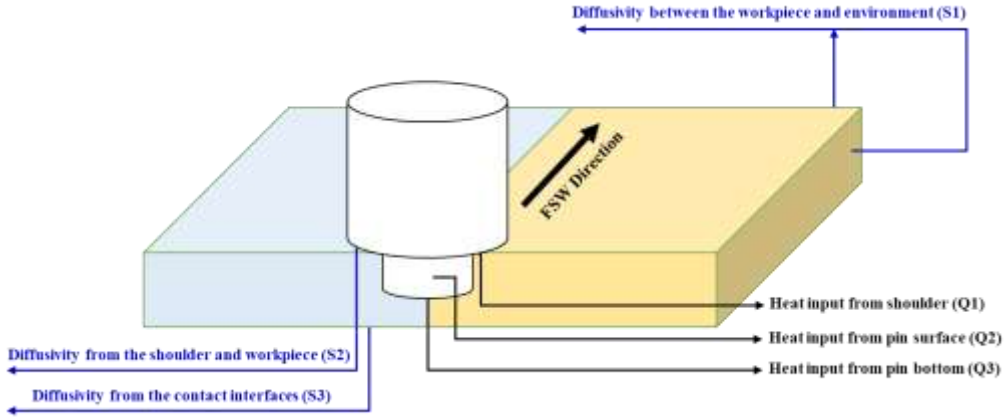

FIGURE 2 Heat inputs and thermal diffusivity locations in the FSW process

The present work neglected the first and third parts: heat generated by material shear (Q1) and heat generated by friction on the bottom surface of the pin (Q3). The heat generated by friction on the lateral surface of the pin (Q2) is calculated from[22]:

$$q_p = \frac{2\mu\overline{Y}r_p HV_{rp}}{\sqrt{3(1+C_f^2)}} \tag{2}$$

Where, $\overline{Y}$ is the average shear stress of the material, r_p is the diameter of the tool pin, HV_{rp} is the thickness of the workpiece being welded, μ is the coefficient of friction , and C_f is the coefficient of friction between the workpiece and the shoulder. The heat input from the shoulder-workpiece interface is estimated as follows [22]:

$$q_s = 2\pi c_f F_n R_i \omega \tag{3}$$

Where R_i is the distance between the tool's rotation axis and a point at the interface below the shoulder, ω is rotational tool speed, and F_n is vertical plunge or thrust force.

Boundary Conditions

The heat transfer and thermal diffusivity between the workpiece and surrounding environment (S1) is a convective heat convection coefficient of h∞. The equation describing this condition on the surface (S1) is written as follows[24]:

$$k\frac{\partial T}{\partial N}\Big|_{\Gamma} = h_{\infty}(T - T_0) \tag{4}$$

The heat transfer boundary conditions at the shoulder and workpiece interface (S2) are given by equations (5) and (6), respectively, as stated in [24]. The first equation shows that the heat transfer from the interface between the workpiece and the shoulder is equal to the product of thermal conductivity and the normal temperature derivative concerning the boundary. In contrast, the second equation shows that the heat transfer from the interface between the pin and the workpiece being welded equals the product of thermal conductivity and the normal temperature derivative concerning the boundary.

$$k\frac{\partial T}{\partial N}\Big|_{\Gamma} = q_s \tag{5}$$

$$k\frac{\partial T}{\partial N}\Big|_{\Gamma} = q_p \tag{6}$$

The qp and qs are calculated from equations (2) and (3). The heat transfer at the contact interface (S3) (bottom surface of the plate and the anvil is given by [24]:

$$k\frac{\partial T}{\partial N}\Big|_{\Gamma} = \overline{h}(T - T_0) \tag{7}$$

Since the two parts being welded are symmetrical, it is assumed that the temperature gradient along a transverse direction to welding is zero along this plane [24]:

$$k\frac{\partial T}{\partial N}\Big|_{\Gamma\ \ sym} = 0 \tag{8}$$

The initial temperature when the tool penetrates the part to be welded is:

$$T(x, y, z, 0) = T_i = 420K \tag{9}$$

MATERIALS AND EXPERIMENTAL PROCEDURE

The FSW process was carried out on a CNC vertical milling machine, using AA6060-T5 sheets with 150 x 40 x 4 mm dimensions. The FSW tool was made of HCHCr steel. Fig. 3 illustrates the FSW tool used, which included a 14 mm diameter shoulder and a 6 mm diameter threaded pin with a height of 3.6 mm. The chemical composition and mechanical properties of the AA6060-T5 alloy are shown in Tables 1 and 2, respectively, while Table 3 indicates the chemical composition of the FSW tool. The heat input was modeled as a function of significant FSW process parameters, and the thermal diffusivity of the material being stirred was analyzed. The temperature was monitored at the contact zone between the FSW tool and the joined sheets using an IR thermometer, a widely used technique to ensure that the welding process was carried out within the appropriate temperature range for the materials being welded.

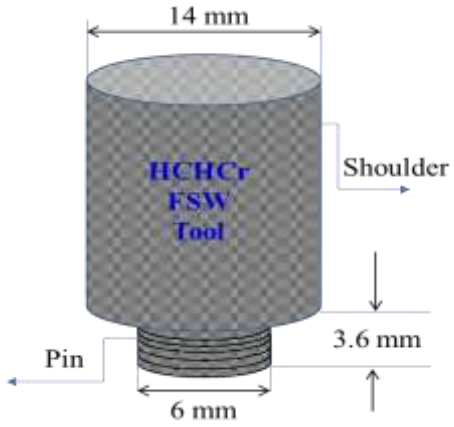

FIGURE 3. FSW tool dimensions

TABLE 1. Typical chemical composition of AA6060-T5 (wt.%)

Element	Fe	Mg	Si	Cr	Cu	Mn	Zn	Ti
%	0.2	0.42	0.39	0.05	0.10	0.10	0.15	0.10

TABLE 2. Mechanical and physical properties of AA6060-T5

E (MPa)	A (%)	ν	Cp (J/Kg °C)	λ (W/m °C)	ρ(g/cm3)	Fusion T(°C)
69500	150	14	200	640	0.33	2.70

TABLE 3. HCHCr tool material chemical composition (wt. %)

Mn	Si	C	S max	P max	Cr
0.52	0.35	2.04	0.03	0.03	11-13

RESULTS AND DISCUSSIONS

Thermal Field

The modelled equations were solved by using three different numerical methods, Gauss, Jacobi, and SOR, respectively, using MATLAB. The obtained results were comparable to those in Fig. 4. This indicates that the model is reliable:

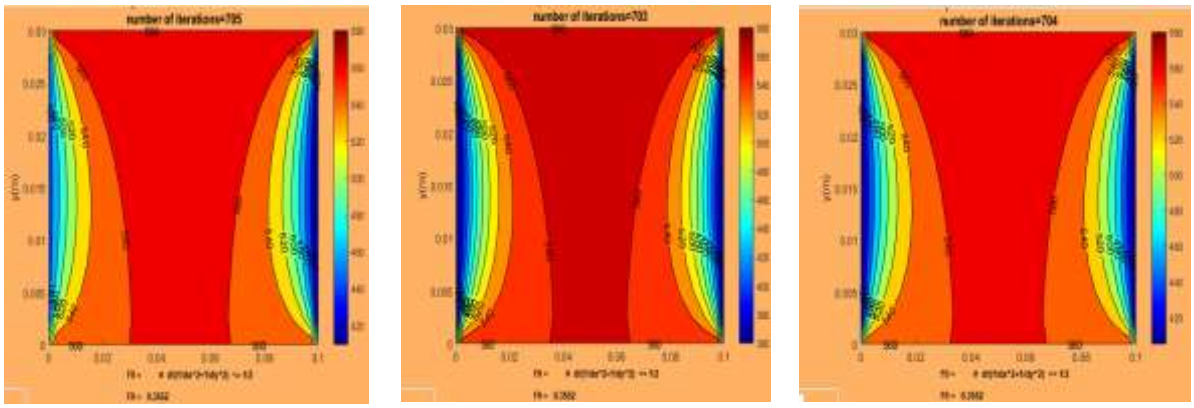

(a) Gaussian (b) Jacobian (c) SOR

FIGURE 4. The thermal diffusivity of the Al AA6060-T5 using a) Gaussian, b) Jacobian, and c) SOR

Figs. 4(a), (b), and (c) show temperature profiles computed through the tool axis and at the workpiece's top surface using the three methods, respectively. It can be noted that the results of the three methods give similar behaviour in thermal diffusivity. For an axial load of 5kN, the temperature reaches a maximum of 580K in the stirring zone. The temperature distribution and the thermal evolution start from the centre of the heating interfaces (source zone). The simulated results have explained the behaviour of generated heat and evolved temperature, which is different around the FSW tool directions, where it is higher behind the tool. Regions close to the heat source are subject to high-temperature gradients. The network of isotherms is symmetrical around the axis perpendicular to the tool's movement. That means the temperature increases (the heating phase) in both directions.

Thermal Diffusivity Field

Thermal diffusivity represents a material's capacity to transfer heat from the hot to cold parts and influences various weld zones' mechanical and metallurgical characteristics. The change in thermal conductivity, density, specific heat, and thermal diffusivity during welding can be seen in Fig. 5, which shows how these properties vary with temperature.

The variation was done in interpolations form to realize the variations of three parameters (i.e., k, ρ, Cp) and their ratio (α). The density in the weld zone decreases slightly with the increase in temperature, manifested in the form of softening of the material (Fig. 5a). Thermal conductivity is found to decrease in the weld region with increasing temperature. This is contrary to the general fact that it increases with temperature. These results (Fig. 5b) may be attributed to the fact that the material being stirred during FSW is under dynamic recrystallization, which

causes simultaneous refinement, deformation and recovery. As the temperature increases, there is an increase in specific heat (Fig. 5c). Thermal diffusivity refers to the rate of heat transfer by conduction. It is also the ratio between conducted heat/stored heat (as in Fig. 5d). Its decrease results in a good weld bead because the HAZ may undergo lesser grain coarsening. During the FSW welding process, AA6061-T6 experiences plastic deformation, leading to a significant decrease in thermal diffusivity, dropping by more than 60% between the temperatures of 385° C and 560 °C.

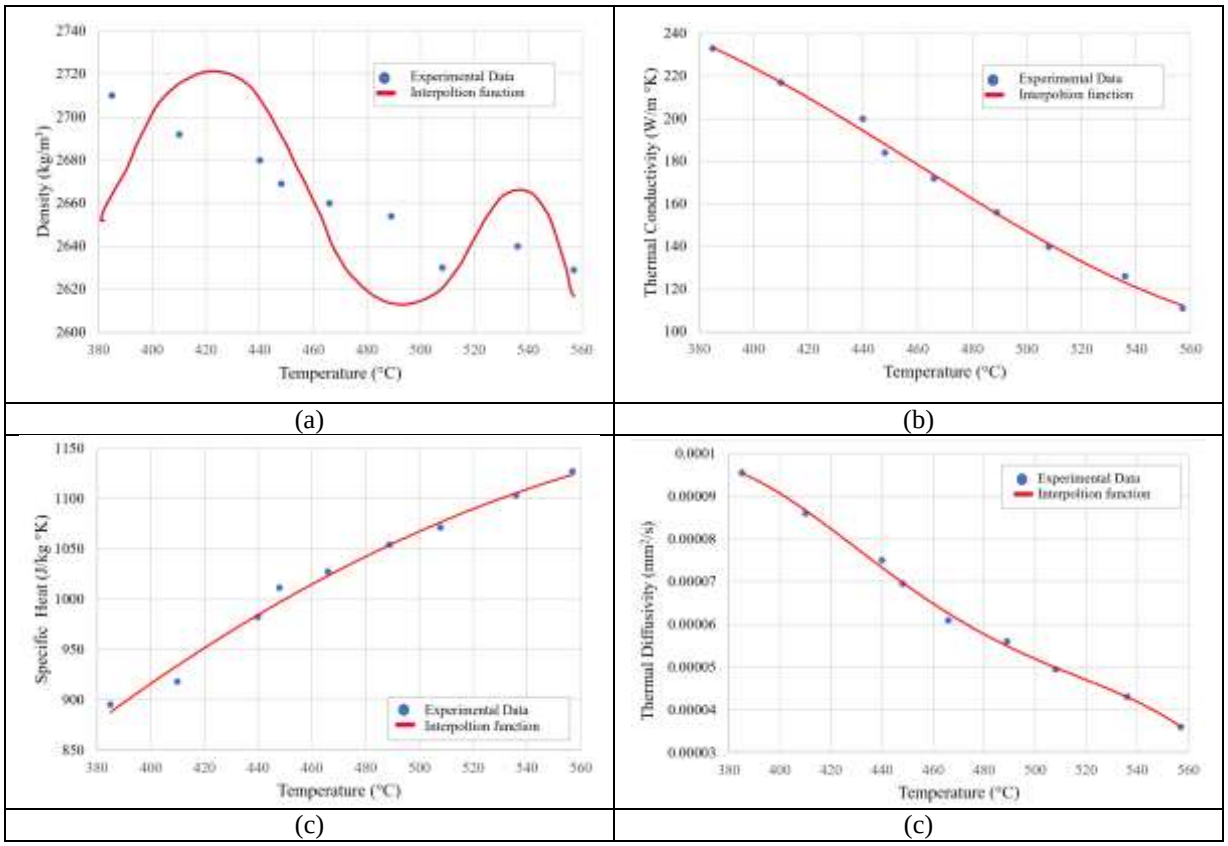

FIGURE 5. effect of temperature on thermal diffusivity of the material being stirred (a) on the density of the, (b) thermal conductivity, (c) Specific heat and (d)ratio of heat conducted to heat stored.

CONCLUSIONS

The primary aim of this study was to comprehend and simulate the FSW stir welding process, specifically focusing on thermal diffusion. This paper used a static 3D model in a moving coordinate system, and the following findings were obtained concerning the heat transfer phenomenon during FSW friction welding:

1. The model utilized in this study enables the precise simulation of the heat transfer phenomenon in the FSW process.
2. The density and thermal conductivity in the weld zone experiences a slight decrease with increasing temperature, while the specific heat increases with increasing temperature.
3. At an equal forging force of 5 KN, the temperature under the tool shoulder can approach the melting temperature of A 6060-T5 aluminum. Due to friction between the tool and workpieces, the specific heat increases with increasing temperature.
4. Thermal diffusivity must be reduced to achieve a good weld joint, which can be achieved by maintaining the melting temperature of the metal in the HAZ zone.

5. During the FSW process, AA6061-T6 undergoes plastic deformation, which causes a substantial reduction in thermal diffusivity. This reduction amounts to more than 60% between 385°C and 560°C.

Finally, according to the critical role of thermal diffusivity in achieving good FSW joints, future studies could focus on developing strategies to control and optimize thermal diffusivity, including using advanced cooling strategies or novel process control approaches.

REFERENCES

1. R. Al-Sabur, "Tensile strength prediction of aluminium alloys welded by FSW using response surface methodology–Comparative review," *Materials Today: Proceedings*, vol. 45, pp. 4504-4510, 2021, doi: 10.1016/j.matpr.2020.12.1001.
2. M. Serier *et al.*, "Parametric studies of friction stir welding with tool using a vibrating shoulder," *Materials Today: Proceedings*, 2022, doi: 10.1016/j.matpr.2022.02.136.
3. R. Al-Sabur, A. K. Jassim, and E. Messele, "Real-time monitoring applied to optimize friction stir spot welding joint for AA1230 Al-alloys," *Materials Today: Proceedings*, vol. 42, pp. 2018-2024, 2021, doi: 10.1016/j.matpr.2020.12.253.
4. R. Al-Sabur, H. I. Khalaf, A. Świerczyńska, G. Rogalski, and H. A. Derazkola, "Effects of Noncontact Shoulder Tool Velocities on Friction Stir Joining of Polyamide 6 (PA6)," *Materials*, vol. 15, no. 12, p. 4214, 2022.
5. A. Jacob, S. Maheshwari, A. N. Siddiquee, and N. Gangil, "Improvements in strength and microstructural behaviour of friction stir welded 7475 aluminium alloy using in-process cooling," *Materials Research Express*, vol. 5, no. 7, p. 076518, 2018.
6. T. Khan, D. Bajaj, and A. N. Siddiquee, "Friction stir engineering for fabrication of ultra-refined cunimgzn alloys," *Materials Letters*, vol. 291, p. 129596, 2021.
7. H. I. Khalaf *et al.*, "The Effects of Pin Profile on HDPE Thermomechanical Phenomena during FSW," *Polymers*, vol. 14, no. 21, p. 4632, 2022.
8. H. I. Khalaf, R. Al-Sabur, M. E. Abdullah, A. Kubit, and H. A. Derazkola, "Effects of Underwater Friction Stir Welding Heat Generation on Residual Stress of AA6068-T6 Aluminum Alloy," *Materials*, vol. 15, no. 6, p. 2223, 2022, doi: 10.3390/ma15062223
9. S. Erfantalab, G. Parish, and A. Keating, "Determination of thermal conductivity, thermal diffusivity and specific heat capacity of porous silicon thin films using the 3ω method," *International Journal of Heat and Mass Transfer*, vol. 184, p. 122346, 2022.
10. B. Kulkarni, S. Pankade, S. Andhale, and C. Gogte, "Effect of backing plate material diffusivity on microstructure, mechanical properties of friction stir welded joints: a review," *Procedia Manufacturing*, vol. 20, pp. 59-64, 2018.
11. W. J. Choi, J. D. Morrow, F. E. Pfefferkorn, and M. R. Zinn, "The effects of welding parameters and backing plate diffusivity on energy consumption in friction stir welding," *Procedia Manufacturing*, vol. 10, pp. 382-391, 2017.
12. [12] X. Zhang, B. Xiao, and Z. Ma, "A transient thermal model for friction stir weld. Part I: the model," *Metallurgical and Materials Transactions A*, vol. 42, no. 10, pp. 3218-3228, 2011, doi: 10.1007/s11661-011-0729-5.
13. J.-H. Kim, Y.-R. Lee, H.-J. Park, S. Kim, and S.-B. Jung, "Microstructures and thermal properties of Ag-CNT/Cu composites fabricated by friction stir welding," *Journal of Materials Science: Materials in Electronics*, vol. 31, pp. 2280-2287, 2020.
14. I. Zybin, K. Trukhanov, A. Tsarkov, and S. Kheylo, "Backing plate effect on temperature controlled FSW process," in *MATEC Web of Conferences*, 2018, vol. 224: EDP Sciences, p. 01084.
15. A. K. Singh, P. Sahlot, M. Paliwal, and A. Arora, "Heat transfer modeling of dissimilar FSW of Al 6061/AZ31 using experimentally measured thermo-physical properties," *The International Journal of Advanced Manufacturing Technology*, vol. 105, pp. 771-783, 2019.
16. B. Kulkarni, S. Pankade, S. Tayde, and S. Bhosle, "Corrosion and mechanical aspects of friction stir welded AA6061 joints: Effects of different backing plates," *Journal of Materials Engineering and Performance*, pp. 1-17, 2023.

17. P. Upadhyay and A. P. Reynolds, "Effects of forge axis force and backing plate thermal diffusivity on FSW of AA6056," *Materials Science and Engineering: A*, vol. 558, pp. 394-402, 2012.
18. Ø. Frigaard, Ø. Grong, and O. Midling, "A process model for friction stir welding of age hardening aluminum alloys," *Metallurgical and materials transactions A*, vol. 32, pp. 1189-1200, 2001.
19. M. Song and R. Kovacevic, "Thermal modeling of friction stir welding in a moving coordinate system and its validation," *International Journal of machine tools and manufacture*, vol. 43, no. 6, pp. 605-615, 2003, doi: 10.1016/S0890-6955(03)00022-1.
20. J. P. Cintra Filho, L. Araújo Filho, R. K. Itikava, M. M. d. Silva, and R. A. Perez, "Thermomechanical modelling of FSW process using a cylindrical tool in an aluminum alloy Alclad AA 2024-T3," *Materials Research*, vol. 21, 2018.
21. G. Buffa, J. Hua, R. Shivpuri, and L. Fratini, "A continuum based fem model for friction stir welding—model development," *Materials Science and Engineering: A*, vol. 419, no. 1-2, pp. 389-396, 2006.
22. P. Colegrove, "3 dimensional flow and thermal modelling of the friction stir welding process," 2001.
23. A. Chikh, M. Serier, R. Al-Sabur, A. Siddiquee, and N. Gangil, "Thermal Modeling of Tool-Work Interface during Friction Stir Welding Process," *Russian Journal of Non-Ferrous Metals*, vol. 63, no. 6, pp. 690-700, 2022.
24. M. Song and R. Kovacevic, "Numerical and experimental study of the heat transfer process in friction stir welding," *Proceedings of the Institution of Mechanical Engineers, Part B: Journal of Engineering Manufacture*, vol. 217, no. 1, pp. 73-85, 2003.